

A Real-time Tracking System for *In Vivo* Endofunctional Capsule using Magnetic Sensors*

Nasir Mehmood¹ and Syed Mahfuzul Aziz²

Abstract—This paper presents a real-time magnetic tracking system to be used for tracking an endofunctional capsule intended to aid in the delivery of biomarkers to specific areas in the gastrointestinal (GI) tract. Magnetic technology is chosen due to its significant advantages over others like RF and Ultrasonics. The tracking system is designed to be used with eight magnetic sensors making it less complex than the other proposed systems. The paper describes a new mathematical model which is more accurate than the existing ones, a linear tracking algorithm and system's performance evaluation for three sensor configurations. The algorithm copes with the problem of magnetic field strength drop due to varying orientation of magnet. The minimum average error obtained is 1.37cm/6.85% in a 20x20x20 cm^3 volume for two dimensional sensor configuration.

I. INTRODUCTION

The idea behind the development of an endofunctional capsule is to investigate the causes of variations in the functional properties of the Gastrointestinal(GI) tract [1]. The apparent agents for these functional variations are the Gastrointestinal diseases like *Bowel Cancer* which are growing in the world and cause severe discomfort to the patients. According to a health survey report issued by the Australian Institute of Health and Welfare (AIHW) in 2011, *Bowel Cancer* was the second largest cause of death in 2007 and 2010, constituting about 15% and 19% respectively of the burden due to cancer only [2]. The traditional GI diagnostic instruments like fibre optic endoscope and colonoscope have an average length of about 2.5m while the GI tract is almost 9m long. So, these instruments are unable to examine a considerable portion of the GI tract.

With the advent of wireless endoscopic capsule technology, the examination of the GI tract has become easier and painless. However, the endoscopic capsules reported to date are also unable to examine the functional changes in the GI tract. This deficiency may be removed by the endofunctional capsule which will be capable of delivering biomarkers at the designated areas of the GI tract with an accuracy of 2-3cm. The delivery of biomarkers to these areas will require the information of capsule location in real-time. Although many technologies including RF and Ultrasonic have been used for real-time *in vivo* tracking [1],[3], magnetic technology offers some advantages over those. The main advantage is that the

magnetic signals are not attenuated when they pass through human organs [4]. However, the problem of magnetic field strength drop with the orientation of the magnet, affects the accuracy of the system.

Many magnetic tracking systems have been proposed by researchers [4],[5],[6],[7]. They all utilize a large number of sensors (e.g. 64) often arranged in a two dimensional array. This requires the patient to lie down during the entire examination period. Although the accuracies claimed are in the range of millimetres, the systems are almost impractical to use in real scenario due to their large size, complexity of cables and patient's discomfort. Large number of sensors also increases the overall cost and complexity of the system. In some cases the patient has to remain under huge magnetic coils for many hours until the capsule passes through the GI tract [8].

To address these problems, a real-time 3-D tracking system using only eight magnetic sensors is proposed in this paper. A new nonlinear mathematical model which takes into account the variation of magnetic field strength with distance, has been developed. A new linear computational algorithm is also developed to locate the magnetic marker accurately. For precise real-time tracking, Levenberg-Marquardt nonlinear method along with Delaunay Triangulation is used. The performance of the system has been evaluated using the proposed mathematical model and algorithm with custom designed tracking hardware.

In this paper, we have proposed a magnetic tracking system which is less complex than the others proposed to date. The reduction in complexity is achieved by creating a more accurate mathematical model for field distribution around a permanent magnet, which leads to a large reduction in the number of sensors required for the tracking system.

II. NONLINEAR MATHEMATICAL MODEL

A few models have been developed for magnetic field distribution around a permanent magnet [1],[4],[5],[9],[10],[11], but they are not sufficient to accurately represent the magnetic field strength with varying distance and orientation of the magnet. So, in this paper we have developed a new mathematical model to overcome the deficiencies found in existing models. Suppose a cylindrical magnet is placed in a Cartesian coordinates system in space. As shown in Figure 1, the magnet is located at $P(x,y,z)$ with its orientation vector $H(\theta,\phi)$ while the sensor is placed at $S(X,Y,Z)$ with respect to centre of the coordinates system. The relative distances of the magnet from the sensor and the centre point O are denoted by 'r' and 'd' respectively.

*This work is funded by Australian Research Council

¹N.Mehmood is PhD research student with the School of Electrical and Information Engineering, University of South Australia, SA 5095, Australia mehny005 at mymail.unisa.edu.au

²S.M.Aziz is Associate Professor with the School of Electrical and Information Engineering, University of South Australia, SA 5095, Australia mahfuz.aziz at unisa.edu.au

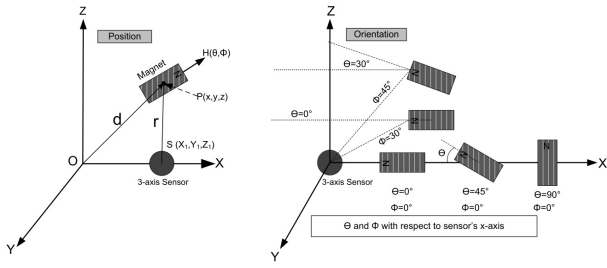


Fig. 1: Position and Orientation of a magnet in space

The magnetization M of the magnet is calculated as

$$M = Flux \times \frac{L}{\sqrt{4 \times (L^2 + \alpha^2)}} \quad (1)$$

Where α is the diameter and L is the length of the magnet, both in millimetres. In order to find the characteristic curve of the magnet, we have performed various experiments using a permanent magnet (12mm×6mm) and a magnetic sensor for $0^\circ, 30^\circ, 45^\circ, 60^\circ, 75^\circ$ and 90° orientations (for $\phi=0$) of the magnet as shown in Figure 1. The measured values of magnetic field densities (B) are plotted versus distance as shown in Figure 2. It is obvious from the graph in Figure

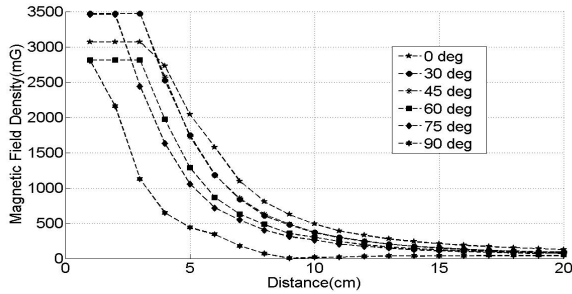


Fig. 2: Magnetic field vs distance for various orientations

2 that there is a gradual variation in received magnetic field density for orientations of the magnet upto 75° . However, there is an abrupt drop in magnetic field strength if the orientation of the magnet is 90° with respect to the sensor. It is clear that the received magnetic field density (B) is nonlinearly and exponentially related to the distance (r) as

$$B \propto \frac{1}{r^N} \text{ and } B \propto e^{-\frac{1}{r^3}} \quad (2)$$

The value of 'N' defines the level of nonlinearity. The received magnetic field strength is also a function of azimuth angle θ and elevation angle ϕ of the magnetic orientation vector H .

$$B \propto \cos(\theta) \cdot \cos(\phi) \quad (3)$$

Combining 2 and 3, we obtain the following relationship

$$B = (K_1 \times M \times \frac{1}{r^N} \times e^{-\frac{1}{r^3}}) \cdot \cos(\theta) \cdot \cos(\phi) \quad (4)$$

Where K_1 is a constant whose value is determined empirically for different orientations of the magnet. Figure 3(a) shows the plot of Equation 4 with 'N' as a parameter and $\theta =$

$\phi = 0$. The suitable value of 'N' is determined statistically by obtaining the RMS percentage errors between the original and modelled values of the magnetic field densities as shown in Figure 3(b). Figures 3(c) and (d) show the dependence of B upon angles θ and ϕ . It is obvious from Figure 3(b)

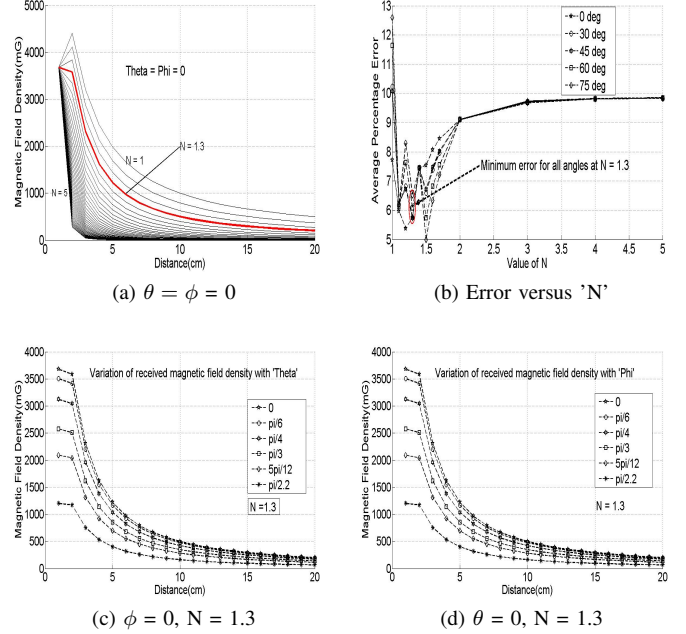


Fig. 3: Graphical plot of proposed model

that minimum error is obtained for $N = 1.3$ for almost all orientations except 90° . We have used Levenberg-Marquardt nonlinear method available in MATLAB as *fsolve* function, to solve Equation 4 which can also be written in the form of a two-variable function F as

$$F(B, r) = r^3 - abs(\frac{1}{\ln[\frac{B_r}{K_1 \times M} \cdot r^N]}) \quad (5)$$

The LM method provides the global minimum value of this function to satisfy the equation based upon a good initial guess. Each sensor measures the values of B_x, B_y and B_z to calculate the resultant magnetic field B , its azimuth angle θ and elevation angle ϕ by Equations 6, 7 and 8 respectively.

$$|B| = \sqrt{B_x^2 + B_y^2 + B_z^2} \quad (6)$$

$$\theta = \arctan(B_y/B_x) \quad (7)$$

$$\phi = \arccos(B_z/|B|) \quad (8)$$

The distance 'r' between the magnet and the sensor, can be calculated as

$$|r| = \sqrt{(x - X)^2 + (y - Y)^2 + (z - Z)^2} \quad (9)$$

III. TRACKING ALGORITHM

Assume that there are N 3-axis magnetic sensors located at positions (X_i, Y_i, Z_i) ($i = 1, 2, \dots, M$). Each sensor provides the values of three orthogonal components of magnetic field density B_x, B_y and B_z , the resultant of which is calculated using Equation 6. Using Equation 4, the respective distances between the magnet and all sensors are calculated. The distances seen by the sensors 1, 2 and 3 can be written as

$$r_1 = \sqrt{(x - X_1)^2 + (y - Y_1)^2 + (z - Z_1)^2} \quad (10)$$

$$r_2 = \sqrt{(x - X_2)^2 + (y - Y_2)^2 + (z - Z_2)^2} \quad (11)$$

$$r_3 = \sqrt{(x - X_3)^2 + (y - Y_3)^2 + (z - Z_3)^2} \quad (12)$$

where, x,y and z are the unknown coordinates of the magnetic marker. Taking squares on both sides of the Equations 10, 11 and 12, we obtain

$$r_1^2 = (x - X_1)^2 + (y - Y_1)^2 + (z - Z_1)^2 \quad (13)$$

$$r_2^2 = (x - X_2)^2 + (y - Y_2)^2 + (z - Z_2)^2 \quad (14)$$

$$r_3^2 = (x - X_3)^2 + (y - Y_3)^2 + (z - Z_3)^2 \quad (15)$$

Subtracting Equation 14 from 13, 15 from 14 and 15 from 13, and then rearranging the interim equations we obtain the following equations respectively.

$$K_{x_{12}}^- x + K_{y_{12}}^- y + K_{z_{12}}^- z = K_{12} \quad (16)$$

$$K_{x_{23}}^- x + K_{y_{23}}^- y + K_{z_{23}}^- z = K_{23} \quad (17)$$

$$K_{x_{31}}^- x + K_{y_{31}}^- y + K_{z_{31}}^- z = K_{31} \quad (18)$$

where, all the constants are as follows.

$$K_{x_{12}}^- = X_2 - X_1, \quad K_{y_{12}}^- = Y_2 - Y_1, \quad K_{z_{12}}^- = Z_2 - Z_1$$

$$K_{x_{23}}^- = X_3 - X_2, \quad K_{y_{23}}^- = Y_3 - Y_2, \quad K_{z_{23}}^- = Z_3 - Z_2$$

$$K_{x_{31}}^- = X_1 - X_3, \quad K_{y_{31}}^- = Y_1 - Y_3, \quad K_{z_{31}}^- = Z_1 - Z_3$$

$$K_{12} = 0.5[K_{r_{12}} - K_{x_{12}}^- \cdot K_{x_{12}}^+ - K_{y_{12}}^- \cdot K_{y_{12}}^+ - K_{z_{12}}^- \cdot K_{z_{12}}^+]$$

$$K_{23} = 0.5[K_{r_{23}} - K_{x_{23}}^- \cdot K_{x_{23}}^+ - K_{y_{23}}^- \cdot K_{y_{23}}^+ - K_{z_{23}}^- \cdot K_{z_{23}}^+]$$

$$K_{31} = 0.5[K_{r_{31}} - K_{x_{31}}^- \cdot K_{x_{31}}^+ - K_{y_{31}}^- \cdot K_{y_{31}}^+ - K_{z_{31}}^- \cdot K_{z_{31}}^+]$$

$$K_{r_{12}} = r_2^2 - r_1^2, \quad K_{r_{23}} = r_3^2 - r_2^2, \quad K_{r_{31}} = r_1^2 - r_3^2$$

$$K_{x_{12}}^+ = X_2 + X_1, \quad K_{y_{12}}^+ = Y_2 + Y_1, \quad K_{z_{12}}^+ = Z_2 + Z_1$$

$$K_{x_{23}}^+ = X_3 + X_2, \quad K_{y_{23}}^+ = Y_3 + Y_2, \quad K_{z_{23}}^+ = Z_3 + Z_2$$

$$K_{x_{31}}^+ = X_1 + X_3, \quad K_{y_{31}}^+ = Y_1 + Y_3, \quad K_{z_{31}}^+ = Z_1 + Z_3$$

Equations 16, 17 and 18 form a set of nonhomogeneous algebraic equations having three unknown variables x, y and z. These equations can be written and solved using matrices as follows.

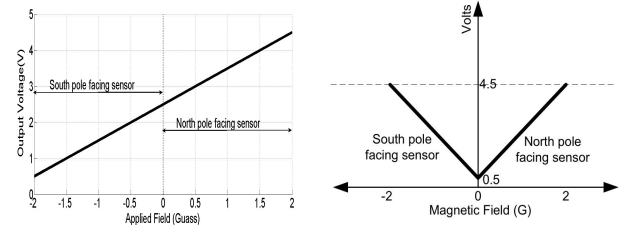
$$\begin{bmatrix} K_{x_{12}}^- & K_{y_{12}}^- & K_{z_{12}}^- \\ K_{x_{23}}^- & K_{y_{23}}^- & K_{z_{23}}^- \\ K_{x_{31}}^- & K_{y_{31}}^- & K_{z_{31}}^- \end{bmatrix} \cdot \begin{bmatrix} x \\ y \\ z \end{bmatrix} = \begin{bmatrix} K_{12} \\ K_{23} \\ K_{31} \end{bmatrix} \quad (19)$$

Solving Equation 19 for the variables x,y and z, the coordinates of the magnetic marker are obtained. Using the same method starting from Equation 10, similar matrix

equations are obtained for all adjacent troika of sensors (2,3,4), (3,4,5), (4,5,6), (5,6,7) and (6,7,8). So, we obtain six different solutions of the variables (x,y,z). At this point, we utilize triangulation method to obtain the mean coordinates. The problem of voltage drop due to magnet's pole reversal is resolved by virtually transforming the transfer function of HMC2003 magnetic sensor using Equation 20 as shown in Figure 4. This transformation will ensure that the calculations are independent of polarity of magnetic field and dependent on field magnitude only.

$$V = \text{absolute}((1 \times \text{data} \times 15.68\text{mV}) - 2.5\text{V}) \quad (20)$$

The values of orientation vector (θ and ϕ) are also calculated



(a) HMC2003 transfer function[12]

(b) New transfer function

Fig. 4: Transfer function transformation

from each sensor's readings using Equations 7 and 8. These values are used to adjust the characteristic curve accordingly. These adjustment values are derived from the graph in Figure 2 and shown in Table I.

TABLE I: Orientation adjustment values

Orientation Angle	Adjustment Value
$0^\circ \leq (\theta, \phi) < 20^\circ$	0%
$20^\circ \leq (\theta, \phi) < 35^\circ$	20.3%
$35^\circ \leq (\theta, \phi) < 50^\circ$	19.14%
$50^\circ \leq (\theta, \phi) < 65^\circ$	35.60%
$65^\circ \leq (\theta, \phi) < 80^\circ$	40.34%
$80^\circ \leq (\theta, \phi) \leq 90^\circ$	75.95%

The proposed algorithm provides a linear solution to the problem of magnetic marker tracking. This algorithm is simpler in computations as compared to those presented in [4],[9],[10] etc.

IV. EXPERIMENTAL RESULTS

The complete tracking system is tested in a $20 \times 20 \times 20 \text{ cm}^3$ volume for three different sensor configurations using eight HMC2003 magnetic sensors and a $12\text{mm} \times 6\text{mm}$ permanent magnet as shown in Figures 5 and 6. For each configuration, the system is tested for 60 random locations of the marker inside the measurement volume with random orientations. Some locations are chosen to be out of measurement plane in each configuration. The error is calculated as the difference between the actual and the measured distances with reference to the centre of coordinates. The average errors for each configuration are calculated to be 1.63cm/8.2%, 1.37cm/6.85% and 2.08cm/10.4% respectively. The error plots for the three configurations are shown in Figure 7.

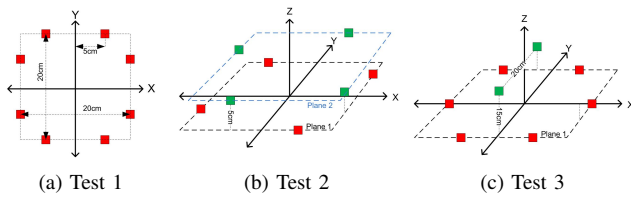


Fig. 5: Position of sensors during testing

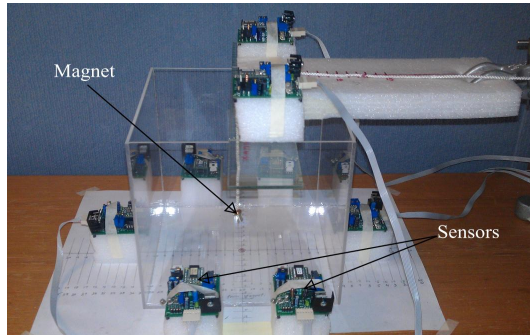


Fig. 6: Experimental setup

V. PERFORMANCE COMPARISON

The *in vivo* tracking systems are compared on the basis of accuracy, cost, complexity, portability, patient's comfort etc. The average error claimed in [1] is 1cm/10% with 3 sensors while the same in our system is 1.37cm/6.85% with 57% less volume of magnet used and 8 times bigger measurement volume. Our results are also better than those presented in [4] in which the average error with ten sensors is more than 15%. In [6], the average error claimed is 10% with 60 magnetic sensors. In terms of cost, portability and patient's comfort, our system has got an upper hand to those presented in [4],[5],[6],[7],[11] and [13], in which 16 to 80 magnetic sensors are used increasing the overall cost and complexity. Our proposed mathematical model is more accurate than the models used in other systems thus enabling us to use much fewer magnetic sensors than other existing magnetic tracking systems. Although the proposed system provides less tracking accuracy compared to some of other systems, the latter use inhibitingly large number of sensors while our proposed system is less complex and therefore

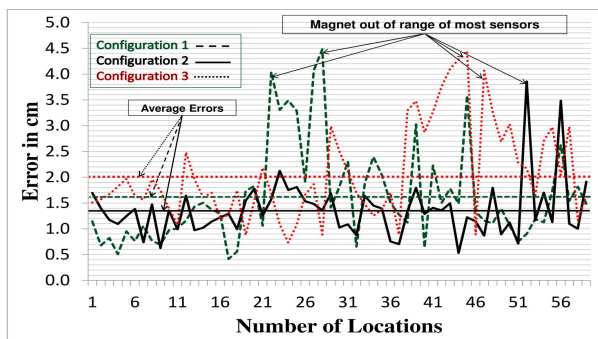


Fig. 7: Error plots for three configurations

practically usable with a tracking accuracy good enough for an endoscopic capsule.

VI. CONCLUSIONS

An *in vivo* magnetic tracking system with eight magnetic sensors has been developed. The paper presents a new mathematical model of the field distribution around a permanent magnet. The model accurately describes the relationship between the magnetic field density and distance between the magnet and the sensor. This has enabled us to develop a simple linear tracking algorithm and ultimately develop a less complex tracking system as compared to other proposed ones. The complete system is tested for three different sensor arrangements. The minimum average error obtained is 1.37cm/6.85% in a $20 \times 20 \times 20\text{cm}^3$ volume when all the sensors are placed in two different 2D planes. The accuracy is reasonable for *in vivo* targeted drug delivery in the GI tract.

REFERENCES

- [1] S. M. Aziz, M. Grcic, and T. Vaithianathan, *A Real-Time Tracking System for an Endoscopic Capsule using Multiple Magnetic Sensors*. Berlin, Heidelberg: Springer Berlin Heidelberg, 2008, vol. 20, pp. 201–218.
- [2] AIHW, "Australian health 2010 available at www.aihw.gov.au/workarea/downloadasset.aspx?id=6442452962 pp 134-140," Australian Institute of Health and Welfare, Tech. Rep., 2010.
- [3] K. Arshak and F. Adepoju, "Capsule tracking in the gi tract: a novel microcontroller based solution," in *Proceedings of the IEEE Sensors Applications Symposium, 2006.*, 2006, pp. 186–191.
- [4] M. Li, C. Hu, S. Song, H. Dai, and M.-H. Meng, "Detection of weak magnetic signal for magnetic localization and orientation in capsule endoscope," in *IEEE International Conference on Automation and Logistics, 2009. ICAL '09.*, aug. 2009, pp. 900–905.
- [5] C. Hu, M.-H. Meng, M. Mandal, and X. Wang, "3-axis magnetic sensor array system for tracking magnet's position and orientation," in *The Sixth World Congress on Intelligent Control and Automation, 2006. WCICA 2006.*, vol. 2, 0-0 2006, pp. 5304–5308.
- [6] C. Peng, J. He, X. Wu, X. Fang, X. Zheng, and W. Hou, "Wearable magnetic locating and tracking system for mems medical capsule," *SENSORS AND ACTUATORS A-PHYSICAL*, vol. 141, no. 2, pp. 432–439, 2007.
- [7] J. Ren, M. Li, C. Hu, L. Yang, S. Song, and M.-H. Meng, "Design of a data acquisition system on magnetic signal for magnetic localization and orientation system," in *8th World Congress on Intelligent Control and Automation (WCICA), 2010*, july 2010, pp. 2142–2147.
- [8] F. Carpi, "Magnetic capsule endoscopy: the future is around the corner," *EXPERT REVIEW OF MEDICAL DEVICES*, vol. 7, no. 2, pp. 161–164, 2010.
- [9] C. Hu, W. Yang, D. Chen, M. Q.-H. Meng, and H. Dai, "An improved magnetic localization and orientation algorithm for wireless capsule endoscope," in *Engineering in Medicine and Biology Society, 2008. EMBS 2008. 30th Annual International Conference of the IEEE*, aug. 2008, pp. 2055–2058.
- [10] X. Wang, M. Meng, and C. Hu, "A localization method using 3-axis magnetoresistive sensors for tracking of capsule endoscope," in *28th Annual International Conference of the IEEE Engineering in Medicine and Biology Society, 2006. EMBS '06.*, sept 2006, pp. 2522–2525.
- [11] K. Yu, G. Fang, and E. Dutkiewicz, "Position and orientation accuracy analysis for wireless endoscope magnetic field based localization system design," in *IEEE Wireless Communications and Networking Conference (WCNC), 2010*, april 2010, pp. 1–6.
- [12] *Online datasheet Honeywell magnetic sensor HMC2003*, Available from <http://www.magneticsensors.com/literature.php>, Feb 2012.
- [13] C. Hu, T. Ma, and M.-H. Meng, "Sensor arrangement optimization of magnetic localization and orientation system," in *IEEE International Conference on Integration Technology, 2007. ICIT '07.*, march 2007, pp. 311–315.